25th ABCM International Congress of Mechanical Engineering
October 20-25, 2019, Uberlândia, MG, Brazil

EXPERIMENTAL STUDY ON CELLULAR INSTABILITY FOR SYNGAS MIXTURES UNDER ATMOSPHERIC AND ELEVATED PRESSURES

Loreto Pizzuti
Federal University of ABC, UFABC, Av. dos Estados, 5001, Santo André – 09210-580, Brazil
loreto.pizzuti@ufabc.edu.br

Cristiane Aparecida Martins
Leila Ribeiro dos Santos
Pedro Teixeira Lacava
Aeronautics Institute of Technology - ITA, São José dos Campos, SP, Brazil, 12228-900
cmartins@ita.br, leila@ita.br, placava@ita.br

Abstract. *This study experimentally determines how the cellular instabilities of syngas mixtures are affected by the simultaneous variation of composition, equivalence ratio and initial pressure. The experimental data of laminar burning velocity is obtained using a cylindrical constant-volume vessel with optical access and schlieren photography. The variables investigated are the initial pressure ranging from 1 to 5 bar, the ratios CO/H2, CO/CH_4 ranging from 0.5 to 2 and the dilution ratio using CO_2 and N_2 ranging from 20 to 60 %. Other variables investigated are the fuel/oxidizer equivalence ratio and the CO_2/N_2 ratio ranging from 0.7 to 1.1 and 0.33 to 3, respectively. The influence of composition on the cellular instability is taken into account considering the effective Lewis number (Le_{Eff}), the thermal expansion ratio and the flame thickness. The expected results will show which parameter or combination of parameters more strongly influence the appearance of cellular instabilities.*

Keywords: *Cellular instability; syngas; laminar burning velocity; constant volume vessel.*

1. INTRODUCTION

In outwardly propagating flames (OPF), the development of cellular instabilities leads to an increase in flame propagation speed and thus an enhanced laminar burning velocity value, S_u^0. Cellular instabilities are caused by thermo-diffusive and hydrodynamic instabilities. Thermo-diffusive instabilities are associated with a Lewis number which is lower than unity or negative values of Markstein length, while hydrodynamic instabilities develop when the ratio between thickness and radius of the flame decreases, independently of the Lewis number (Chen, 2015). According to the literature (Egolfopoulos et al., 2014; Matalon, 2006) thermo-diffusional cellular instabilities and hydrodynamic instabilities may affect the flame front evolution. The thermo-diffusional instabilities develop for Lewis number Le < 1 and larger flame radius where the stretch rate is small. Hydrodynamic instabilities could develop for any Le value as the flame thickness decreases, which is the case for most mixtures where the initial pressure or the flame radius increase, and when the thermal expansion ratio increases which is the case when the equivalence ratio is close to unity.

Cellular instabilities have been visualized since the 80's. Groff, (1982) was one of the first researchers to record the flame evolution using high speed schlieren photography with film of 500 frames per second (fps). The onset of the cellular flames was found to correspond to a critical flame Reynolds number which is a function of the flame expansion ratio. It appears that the observed cellular flames are caused by hydrodynamic instability mechanisms for propane air mixtures at ambient temperature and pressure between 200 and 500 kPa and equivalence ratios in the range of 0.7-1.0.

Cellular instabilities in iso-octane/air and mixtures of iso-octane-n-heptane/air were investigated by Bradley et al. (1998). It was found that a small Markstein length is indicative of both a small influence of flame stretch rate on burning velocity and an earlier onset of instabilities. At higher pressures and temperatures, flames are more prone to develop a cellular structure, which eventually leads to an increase in flame speed (Bradley et al., 1998). Additionally, the critical Peclet number for the onset of instabilities has been correlated with the Markstein number instead of the Reynolds number.

Most of the earlier researchers investigated cellular instabilities in individual fuels such as CH4, C3H8, H2 burning in air (Bradley & Harper, 1994; Kwon, et.al., 2002). More recently, the interest in syngas, obtained from biomass as a source of energy, has driven the interest of researchers regarding cellular instabilities in such mixtures with multicomponent reactants (fuels). The effects on cellular instability of hydrocarbons addition such as C3H8 to H2 (Law et al., 2005) or CH4, C3H8 and C4H10 to H2/CO have been investigated (Park et al., 2009). Law and coworkers found that a flame, in a lean mixture of hydrogen, with no propane present, is characterized by an effective Lewis number,

Le_{Eff}, less than the critical Le^*_{Eff} and is therefore predicted to be unconditionally unstable. Such instability is due to diffusive-thermal effects. On the contrary, a flame in a lean mixture of propane, with no hydrogen present which has $Le_{Eff} > Le^*_{Eff}$, is predicted to be stable for small radii. The instability that arises when the flame reaches a critical size is hydrodynamic in nature and is due to the thermal expansion of the gas (Law et al., 2005). Vu and coworkers found that with propane and butane additions to H2/CO, the propensity for cell formation was diminished for both hydrodynamic and diffusional–thermal instabilities, whereas the cellular instabilities for methane-added syngas/air flames are not suppressed (Vu et al., 2010).

When considering three biomass derived gases, all with H2/CO/CO2/N2/CH4 species in their composition, Song and coworkers (Song et al., 2011) found that, with hydrogen enrichment, the propensity of destabilization tends to be progressively promoted because of the enhancement of both hydrodynamic and diffusional-thermal instabilities. For carbon monoxide addition, there were no differences in the propensity of destabilization. For methane addition, the flame front instabilities were diminished because of the significant increase in the flame thickness.

H2/CO-air intrinsic instabilities were studied by varying the H2 fractions from 0 to 100% (Li et al., 2014). With hydrogen fractions above 50%, the instability increases for flames of lower hydrogen fractions. For the premixed syngas flame with hydrogen fractions greater than 50%, the decline in cellular instabilities induced by the increase in equivalence ratio can be attributed to a reduction of diffusive-thermal instabilities rather than increased hydrodynamic instability.

By analyzing data obtained using OPF technique coupled with high speed schlieren photography, this paper aims to identify the influences of thermal expansion ratio, flame thickness and mixture Lewis number on the generation of hydrodynamic and diffusional-thermal instabilities leading to the appearance of cells over the flame surface of biomass syngas/CH4 mixtures.

2. PARAMETERS INVOLVED IN THE CELLULAR INSTABILITIES ANALYSIS

For multi-component fuel mixtures, such as in syngas fuel, the effective Lewis number can be determined by different formulations. According to Bouvet et al. (2013) three formulations can be found in the literature, i.e. the heat released based, Eq. (1), volume based Eq. (2) and diffusion based Eq. (3):

$$Le_H = 1 + \frac{q_1\left(Le_1 - 1\right) + q_2\left(Le_2 - 1\right)}{q_1 + q_2} \tag{1}$$

$$Le_V = x_1 Le_1 + x_2 Le_2 \tag{2}$$

$$Le_D = \frac{D_T}{x_1 D_{1/N_2} + x_2 D_{2/N_2}} \tag{3}$$

where q_i is the non-dimensional heat release corresponding to the fuel species i, x_i is the fuel volumetric fraction of the component i, Le_i is the Lewis number of the component i, D_T, the mixture thermal diffusivity and D_{i/N_2}, the mass diffusivity of the deficient fuel species i, conventionally taken as the reactant-inert binary diffusion coefficient. According to Bouvet, the volume based formulation should be preferred when researching lean H_2/HC/air flame stability. In the present research the Le_V formulation is used for the H_2/CO/CH_4/air mixtures analyzed due to its simplicity and validation for lean H_2/CH_4/air mixtures. The formulation considering the Lewis number of the deficient reactant has been used as the overall effective mixture Lewis number. According to this formulation, the overall Le_{eff} is smaller than one for lean mixtures and larger than one for rich mixtures (Matalon, 2006).

The laminar burning velocity S_u^0 has been experimentally determined by using the linear relationship between the flame propagation speed S_b and the stretch rate K given by $S_b^0 = S_b + K\ L_b$ and applying the continuity equation $S_u^0 = \rho_b / \rho_u S_b^0$. The flame propagation speed has been experimentally determined from the flame radius evolution recorded by high speed schlieren photography considering the flame radius evolution between 8 and 18 mm, indicated as lower, R_{fL} and upper flame radius, R_{fU}. For the purpose of comparison, the S_u^0 has been determined using the ChemKin laminar premixed flame code PREMIX using the San Diego mechanism. The S_u^0 determined by simulation is used for flame thickness determination of all mixtures under analysis given by the following equation $\delta = \lambda / c_p / (\rho_u S_u^0)$ where λ and c_p, the thermal conductivity and the specific heat of the mixture, have been evaluated at the freestream composition of the mixture, at 1100 K, which is approximately the average of the freestream and flame temperatures (Law et al., 2005; Vu et al., 2011). The thermal expansion ratio $\sigma = \rho_u / \rho_b$, has been evaluated for all mixtures using the Gaseq program considering the adiabatic temperature and composition at constant pressure.

Figure 1 shows the flame surface of two mixtures, 15 and 3, presenting smooth and cellular instabilities flame surface, respectively.

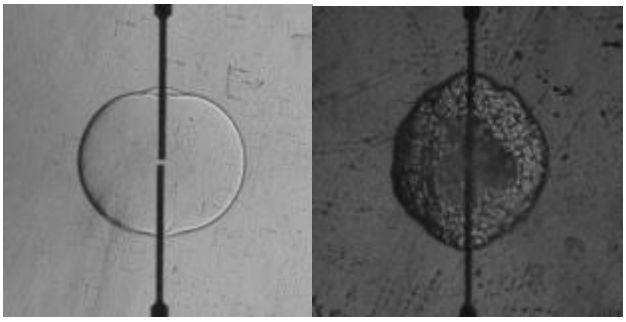

Figure 1. Comparison of flame surface at 18 mm radius for mixtures 15 and 3, respectively.

3. EXPERIMENTAL SETUP

The experimental data are obtained by using the spherical outwardly propagating flame technique in the approximate constant pressure period, just after ignition, coupled with high speed schlieren photography. Therefore, a cylindrical constant volume combustion chamber (CVCC) designed to work with P_0 up to 6 bar has been used. A detailed description of the experimental setup, including the schlieren setup, is presented in Pizzuti et al., (2018) whereas the setup validation is presented in Pizzuti et al. (2017). The syngas mixtures have been prepared in a 20 liter auxiliary cylinder by using the partial pressure technique combining five high purity gases stored in high pressure cylinders, i.e., CO, CO_2, CH_4, H_2, N_2. The quantity of air required to achieve the desired mixture equivalence ratio is added to the syngas already in the auxiliary cylinder by the partial pressure method.

The design of experiments technique (DoE) has been used in order to consider a large number of variables or factors while minimizing the number of experiments. Table 1 presents the matrix of experiments with the 21 syngas mixtures studied in this research. The considered factors are fuel composition, in terms of CH_4/H_2 and CO/H_2, dilution composition (CO_2/N_2), degree of dilution (DoD) that is the percentage of diluents (CO_2 % + N_2 %) in the syngas mixture, initial pressure and equivalence ratio. Each factor has been evaluated at three levels except for ϕ which has four levels. The values for the levels are presented in Tab. 1.

Table 1 – Matrix of experiments for syngas mixtures ($H_2/CO/CO_2/N_2/CH_4$).

N°#	CH_4/H_2	CO/H_2	CO_2/N_2	DoD(%)	P_0(bar)	ϕ
1	0.5	0.5	0.33	60	5	0.5
2	0.5	0.5	1.5	60	3	1.1
3	0.5	0.5	5.0	40	5	0.7
4	0.5	1	0.33	20	3	1.1
5	0.5	1	1.5	40	1	0.7
6	0.5	2	0.33	20	3	0.9
7	0.5	2	1.5	40	5	0.9
8	0.5	2	5.0	60	1	0.5
9	1	0.5	1.5	20	3	0.5
10	1	0.5	1.5	60	1	0.9
11	1	1	0.33	40	1	0.5
12	1	1	5.0	20	5	0.9
13	1	1	5.0	60	3	0.7
14	1	2	0.33	60	3	0.7
15	1	2	5.0	20	1	1.1
16	2	0.5	5.0	40	1	1.1
17	2	0.5	5.0	40	3	0.9
18	2	1	0.33	60	1	0.9
19	2	1	5.0	20	5	0.5
20	2	2	1.5	20	1	0.7
21	2	2	1.5	40	3	0.5

4. RESULTS AND ANALYSIS

This section presents the results of the analysis of the influence of P_0, σ, δ and mixture Le_{Eff} on the generation of hydrodynamic and diffusional-thermal instabilities leading to appearance of cells over the flame surface for syngas/CH_4 mixtures, when the corrected Darrieus-Landau (DL) theory is used in order to explain the experimental results (Addabbo et al., 2007; Matalon, 2006).

Figures 2, 3 and 4 present some syngas/CH_4 mixture properties values for mixtures ignited at P_0 of 1, 3 and 5 bar, respectively. The experiments are performed randomly in order to distribute systematic errors of the system and of the process. Therefore, the mixture number (N° #) is that defined in the DoE matrix. Each of these tables presents the volume percentage of each combustible species in the fuel mixture, ϕ, the experimentally measured and simulated S_u^0, the mixture Le_{Eff}, σ, and δ.

There are two instances at which flame wrinkling changes characteristics. The first is when the large cracks formed from the initial ignition disturbance start to branch and lose similarity, and the second is the spontaneous appearance of cells almost uniformly over the entire surface (Law et al., 2005). The second instance is used as the condition where the flame loses its stability. The analysis of Figs. 2-3 shows that while the flames remain basically smooth at 1 bar in the flame radius range 8-18 mm, they become wrinkled as pressure increases, with the onset of wrinkling occurring earlier for higher pressures.

This trend is explained considering that both thermal and viscous diffusion have stabilizing effects on the flame surface. When P_0 increases, the diffusion length l_f, representing the flame thickness, decreases, and thus reduces the stabilizing effect. This allows wrinkling to occur earlier in time and radius.

4.1 Initial pressure of 1 bar

Considering the mixtures with P_0 = 1 bar presented in Fig. 2, none develops cellular instabilities within the flame radius range 8-18 mm. With the exception of mixture 15, whose flame thickness is 0.12 mm, all other mixtures present quite large values of δ, i.e., $\delta > 0.22$ mm, associated with stability of the flame front. Mixtures 15 and 16 present the highest σ (7.02 and 6.85, respectively) and the smallest δ (0.12 and 0.22 mm, respectively), both parameters associated with the early development of instabilities. However, they present the largest Le_{Eff} (1.185 and 1.150). During the early stages of propagation the hydrodynamic instability is suppressed because of the large curvature of the flame front, and since for high Lewis numbers molecular diffusion exerts stabilizing influences on the short wavelength disturbances, a smooth, stable flame results (Matalon, 2006). However, most mixtures present large cracks formed during spark ignition.

4.2 Initial pressure of 3 bar

Most of mixtures with P_0 = 3 bar presented in Fig. 3 present the beginning of branching and the loss of similarity of the large cracks formed from the initial ignition disturbance in the flame radius range 8-18 mm. This is the case for mixtures 6, 9, 13, 14 and 17, for which large, non-uniformly distributed cells are visible on the flame front at 18 mm. Mixtures 2 and 4 present Le_{Eff} larger than unit (1.21 and 1.27, respectively); therefore, despite the large σ (5.85 and 7.06) and the small δ (0.19 and 0.05 mm) the molecular diffusion exerts stabilizing influences on the short wavelength disturbances. The large cracks formed from the initial ignition disturbance just grow without losing similarity. Mixture 6 and 17 develop non-uniformly distributed cells earlier than mixtures 13 and 14 as the former present lower δ and a higher σ than the latter, both parameters favorable for hydrodynamic instability. All of these mixtures have Le_{Eff} lower than unit. Therefore, both thermo-diffusional and hydrodynamic instabilities affect the flame front evolution, with the hydrodynamic instability controlling the flame front evolution. Weak mixtures 9 and 21, both burning with low flame speeds, are clearly affected by buoyancy, visible as the upward dislocated flame surface at 18 mm. Therefore, the non-spherical flame evolution and the stretch rate affecting the flame front must be taken into account.

N# / V%	CH_4/H_2	CO/H_2	CO_2/N_2	Dil Rate	θ	S_u^0 (cm/s) Measured	S_u^0 (cm/s) (SD)	Le_{Eff} *	σ	δ (mm)	Schlieren Image at 8 mm radius	Schlieren Image at 18mm radius
(5) CH4: 8.6 CO: 25.7 H2: 25.7 CO2: 20.0 N2: 20.0	0.5	1	1	40	0.7	27.73	25.4	0.80	5.7	0.26	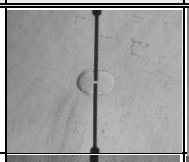	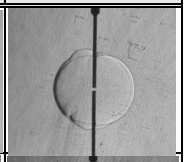
(8) CH4: 3.1 CO: 27.7 H2: 9.2 CO2: 45.0 N2: 15.0	0.5	2	3	60	0.5	4.85	4.85	0.84	4.39	1.22	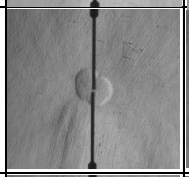	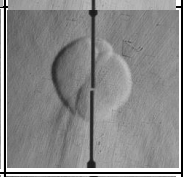
(10) CH4: 17.1 CO: 5.7 H2: 17.1 CO2: 30.0 N2: 30.0	1	0.5	1	60	0.9	18.18	18.9	0.76	6.02	0.33	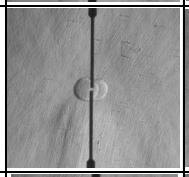	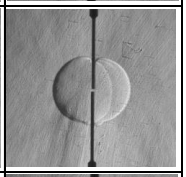
(11) CH4: 20.0 CO: 20.0 H2: 20.0 CO2: 10.0 N2: 30.0	1	1	0.33	40	0.5	7.02	7.86	0.82	4.8	0.8	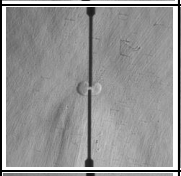	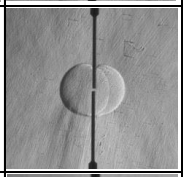
(16) CH4: 16.0 CO: 48.0 H2: 16.0 CO2: 15.0 N2: 5.0	1	2	3	20	1.1	50.62	52.7	118	7.02	0.12	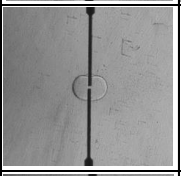	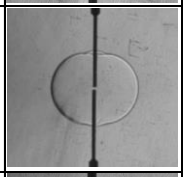
(18) CH4: 41.5 CO: 4.6 H2: 13.8 CO2: 30.0 N2: 10.0	2	0.5	3	40	1.1	28.53	28,00	1.15	6.85	0.22	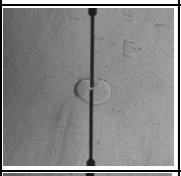	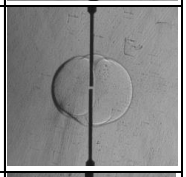
(20) CH4: 24.0 CO: 8.0 H2: 8.0 CO2: 15.0 N2: 45.0	2	1	0.33	60	0.9	17.36	20.9	0.85	6.25	0.3	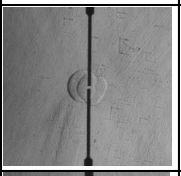	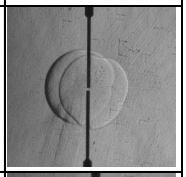
(23) CH4: 34.3 CO: 34.3 H2: 11.4 CO2: 10.0 N2: 10.0	2	2	1	20	0.7	20.73	24.8	0.91	6.05	0.25	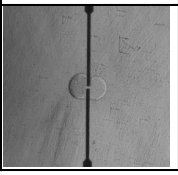	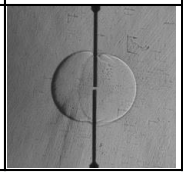

Figure 2 – Syngas/CH_4 mixtures properties at P_0 of 1 bar: mixture number (N°#), equivalence ratio, ϕ, experimentally and simulated value of S_u^0, effective Lewis number, Le_{Eff}, thermal expansion ratio, σ, flame thickness, δ, and images of flame surface at radius of 8 and 18 mm.

N° #	V (%)	CH_4/H_2	CO/H_2	CO_2/N_2	Dil. rate	φ	S_u^0 Exp. (cm/s)	S_u^0 Sim. (cm/s)	Le_{Eff}	σ	δ (mm)	R_{fL} = 8 mm	R_{fU} = 18 mm
2	CH4: 10.0 CO: 10.0 H2: 20.0 CO2: 30.0 N2: 30.0	1/2	1/2	1	60	1.1	13.3	12.0	1.21	5.85	0.19	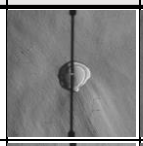	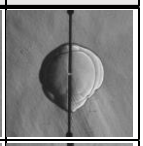
4	CH4: 16.0 CO: 32.0 H2: 32. CO2: 5.0 N2: 15.0	1/2	1	1/3	20	1.1	55.5	47.6	1.27	7.06	0.05	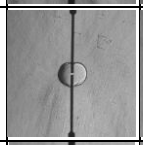	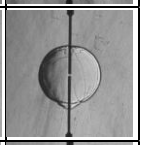
6	CH4: 11.4 CO: 45.7 H2: 22.9 CO2: 5.0 N2: 15.0	1/2	2	1/3	20	0.9	44.1	32.2	0.92	6.79	0.06	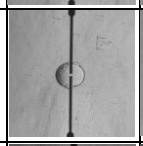	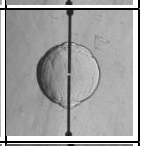
9	CH4: 32.0 CO: 16.0 H2: 32.0 CO2: 10.0 N2: 10.0	1	1/2	1	20	0.5	4.0	3.8	0.76	4.93	0.56	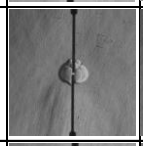	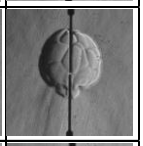
13	CH4: 13.3 CO: 13.3 H2: 13.3 CO2: 45.0 N2: 15.0	1	1	3	60	0.7	7.3	6.0	0.79	5.24	0.33	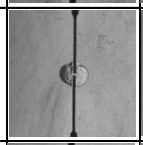	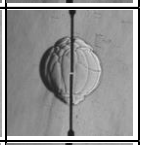
14	CH4: 10.0 CO: 20.0 H2: 10.0 CO2: 15.0 N2: 45.0	1	2	1/3	60	0.7	8.0	8.7	0.89	5.38	0.24	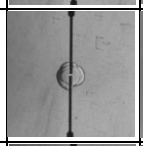	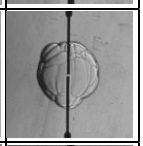
17	CH4: 34.3 CO: 8.6 H2: 17.1 CO2: 30.0 N2: 10.0	2	1/2	3	40	0.9	17.5	16.7	0.82	6.64	0.12	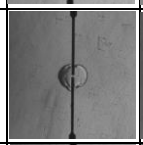	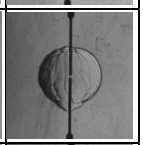
21	CH4: 24.0 CO: 24.0 H2: 12.0 CO2: 20.0 N2: 20.0	2	2	1	40	0.5	0.91	3.1	0.90	4.82	0.64	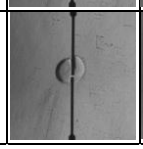	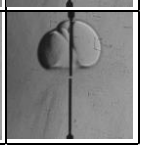

Figure 3 – Syngas/CH_4 mixtures properties at P_0 of 3 and 5 bar: mixture number (N° #), equivalence ratio, ϕ, experimentally and simulated value of S_u^0, effective Lewis number, Le_{Eff}, thermal expansion ratio, σ, flame thickness, δ, and images of flame surface at radius of 8 and 18 mm.

4.3 Initial pressure of 5 bar

Figure 4 presents syngas/CH_4 mixtures with P_0 = 5 bar. With the exception of those clearly affected by buoyancy, these mixtures develop cellular instabilities before reaching the flame radius range 8-18 mm under analysis. Unfortunately, for mixtures 1, 3, 7 and 19 the optical windows suffered wear due to high temperature in the central region where flame ignition occurs. For mixtures 1 and 19, the damaged region is shown in the schlieren images at 18 mm. It follows that the image visualization of the first instants after ignition are not available for such mixtures. However, for mixture 12 the visualization is possible, showing that at 8 mm the flame surface is uniformly covered with cells of almost the same dimensions. In addition, the light source of the schlieren system, a high luminosity LED, reduced its luminosity as consequence of crystal degradation, thereby reducing the schlieren system sensitivity. For mixtures 7 and 12 δ is 0.06 mm and σ is 6.37 and 6.86, respectively, while Le_{Eff} is 0.841 and 0.895, respectively. Therefore, the enhanced hydrodynamic instabilities are modulated by lower diffusional-thermal instabilities when compared with mixture 3 where the reduced hydrodynamic instabilities are enhanced by higher diffusional-thermal instabilities. Mixtures 1 and 19 due to their S_u^0 in the order of 1-2 cm/s, are strongly affected by buoyancy. Therefore, the stretch rate affecting the flame front modifies its geometry, and they cannot be considered when investigating flame front cellular instability.

N° #	V (%)	CH_4/H_2	CO/H_2	CO_2/N_2	Dil. rate	φ	S_u^0 Exp. (cm/s)	S_u^0 Sim. (cm/s)	Le_{Eff}	σ	δ (mm)	R_{fL} = 8 mm	R_{fU} = 18 mm
1	CH4: 10.0 CO: 10.0 H2: 20.0 CO2: 15.0 N2: 45.0	1/2	1/2	1/3	60	0.5	1.3	1.2	0.70	6.00	1.05	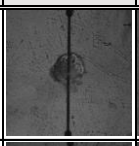	
3	CH4: 15.0 CO: 15. H2: 30.0 CO2: 30.0 N2: 10.0	1/2	1/2	3	40	0.7	13.7	10.8	0.72	5.64	0.12	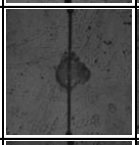	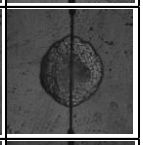
7	CH4: 8.6 CO: 34.3 H2: 17.1 CO2: 20.0 N2: 20.0	1/2	3	1	40	0.9	21.8	20.1	0.89	6.37	0.06	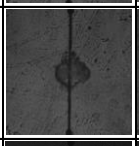	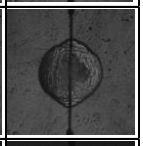
12	CH4: 26.7 CO: 26.7 H2: 26.7 CO2: 15.0 N2: 5.0	1	1	3	20	0.9	27.0	22.8	0.84	6.86	0.06	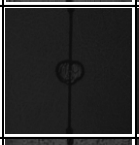	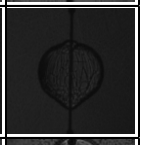
19	CH4: 40.0 CO: 20.0 H2: 20.0 CO2: 15.0 N2: 5.0	2	1	3	20	0.5	0.4	1.9	0.85	4.93	0.63	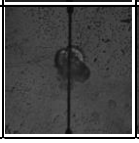	

Figure 4 – Syngas/CH_4 mixtures properties at P_0 of 5 bar: mixture number (N° #), equivalence ratio, ϕ, experimentally and simulated value of S_u^0, effective Lewis number, Le_{Eff}, thermal expansion ratio, σ, flame thickness, δ, and images of flame surface at radius of 8 and 18 mm.

5. CONCLUSIONS

This paper aims to identify the influences of initial pressure, thermal expansion ratio, flame thickness and mixture effective Lewis number on the generation of hydrodynamic and diffusional-thermal instabilities leading to the appearance of cells over the flame surface of synthetic biomass syngas/CH_4 mixtures analyzing experimental data obtained using the OPF technique coupled with high speed schlieren photography. The DoE technique has been used to cover a large number of variables using reduced number of experiments. The variables investigated are P_0 at 1, 3 and 5 bar, the ratios CO/H2, CO/CH_4 at 1/2, 1 and 2 and the dilution ratio (CO_2 + N_2) %, ranging from 20 to 60 %. The other variables investigated are ϕ and the CO_2/N_2 ratio ranging from 0.7 to 1.1 and 1/3 to 3, respectively. The influence of composition on the cellular instability is taken into account considering the Le_{Eff}. The following results have been found when the corrected DL theory is used in order to explain the experimental results:

- Higher P_0 lead to an earlier onset of wrinkling, as a result of a smaller diffusion length l_f, which reduces the stabilizing effect.
- Higher σ leads to an earlier appearance of cells on the flame front. The experiments show that, mixtures with ϕ close to stoichiometry develop hydrodynamic instabilities earlier in time and radius.
- The thermal diffusivity decreases with pressure, suppressing its stabilizing effect on flame front instabilities. Therefore, mixtures with lower diffusivities and δ tend to develop hydrodynamic instabilities earlier in time.
- The experimental results show that mixtures with $Le_{Eff} < 1$ develop cellular instabilities earlier in time and radius compared to mixtures presenting $Le_{Eff} > 1$. These results are explained considering that in the first situation molecular diffusion does not exerts stabilizing effect on the short wavelength disturbances, thus the instability is diffusive-thermal in nature. In the second case molecular diffusion exerts stabilizing effect on the short wavelength disturbances, thus resulting in a more stable flame. In this case, the instability is hydrodynamic in nature, triggered by thermal expansion effects. However, the instabilities are suppressed during the early stages of propagation because of the large curvature of the flame front.

6. ACKNOWLEDGEMENTS

The authors are grateful to the Brazilian federal agency CAPES for the financial support of a four years PhD scholarship and for the Visiting Professor support through PVS 23038.009640/2013-86 project and to FAPESP agency for financially supporting the experimental project through the Process 2010/51315-3.

7. REFERENCES

Addabbo, R., Bechtold, J. K., & Matalon, M. (2007). Wrinkling of spherically expanding flames. *Proceedings of the Combustion Institute*, *29*(2), 1527–1535. https://doi.org/10.1016/s1540-7489(02)80187-0

Bouvet, N., Halter, F., Chauveau, C., & Yoon, Y. (2013). On the effective Lewis number formulations for lean hydrogen/hydrocarbon/ air mixtures. *International Journal of Hydrogen Energy*, *38*(14), 5949–5960. https://doi.org/10.1016/j.ijhydene.2013.02.098

Bradley, D., & Harper, C. M. (1994). The development of instabilities in laminar explosion flames. *Combustion and Flame*, *99*(3–4), 562–572. https://doi.org/10.1016/0010-2180(94)90049-3

Bradley, D., Hicks, R. a., Lawes, M., Sheppard, C. G. W., & Woolley, R. (1998). The Measurement of Laminar Burning Velocities and Markstein Numbers for Iso-octane – Air and Iso-octane – n- Heptane – Air Mixtures at Elevated Temperatures and Pressures in an Explosion Bomb. *Combustion and Flame*, *115*, 126–144.

Chen, Z. (2015). *On the accuracy of laminar burning velocity measured from propagating spherical flames Introduction*. *162*.

Egolfopoulos, F. N., Hansen, N., Ju, Y., Kohse-H??inghaus, K., Law, C. K., & Qi, F. (2014). Advances and challenges in laminar flame experiments and implications for combustion chemistry. *Progress in Energy and Combustion Science*, *43*, 36–67. https://doi.org/10.1016/j.pecs.2014.04.004 Review

Groff, E. G. (1982). The cellular nature of confined spherical propane-air flames. *Combustion and Flame*, *48*(C), 51–62. https://doi.org/10.1016/0010-2180(82)90115-8

Kwon, O. C., Rozenchan, G., & Law, C. K. (2002). Cellular instabilities and self-acceleration of outwardly propagating spherical flames. *Proceedings of the Combustion Institute*, *29*(2), 1775–1783. https://doi.org/10.1016/S1540-7489(02)80215-2

Law, C. K., Jomaas, G., & Bechtold, J. K. (2005). Cellular instabilities of expanding hydrogen/propane spherical flames at elevated pressures: Theory and experiment. *Proceedings of the Combustion Institute*, *30*(1), 159–167. https://doi.org/10.1016/j.proci.2004.08.266

Li, H. M., Li, G. X., Sun, Z. Y., Zhai, Y., & Zhou, Z. H. (2014). Measurement of the laminar burning velocities and markstein lengths of lean and stoichiometric syngas premixed flames under various hydrogen fractions. *International Journal of Hydrogen Energy*, *39*(30), 17371–17380. https://doi.org/10.1016/j.ijhydene.2014.07.177

Matalon, M. (2006). Intrinsic Flame Instabilities in Premixed and Nonpremixed Combustion. *Annual Review of Fluid Mechanics*, *39*(1), 163–191. https://doi.org/10.1146/annurev.fluid.38.050304.092153

Park, J., Lee, D. H., Yoon, S. H., Vu, T. M., Yun, J. H., & Keel, S. I. (2009). Effects of Lewis number and preferential diffusion on flame characteristics in 80%H2/20%CO syngas counterflow diffusion flames diluted with He and Ar. *International Journal of Hydrogen Energy*, *34*(3), 1578–1584. https://doi.org/10.1016/j.ijhydene.2008.11.087

Pizzuti, L., Martins, C. A., & Ribeiro dos Santos, L. (2018). *Experimental determination of laminar burning velocity of biogas at pressures up to 5 Bar*. *17*(2), 3–11. https://doi.org/10.26678/abcm.cobem2017.cob17-0672

Song, W. S., Vu, T. M., Park, J., & Kwon, O. B. (2011). *Measurements of Laminar Burning Velocities and Flame Stability Analysis of Biomass Derived Gas – Air Premixed Flames*.

Vu, T. M., Park, J., Kim, J. S., Kwon, O. B., Yun, J. H., & Keel, S. I. (2011). Experimental study on cellular instabilities in hydrocarbon/hydrogen/carbon monoxide-air premixed flames. *International Journal of Hydrogen Energy*, *36*(11), 6914–6924. https://doi.org/10.1016/j.ijhydene.2011.02.085

Vu, T. M., Park, J., Kwon, O. B., Bae, D. S., Yun, J. H., & Keel, S. I. (2010). Effects of diluents on cellular instabilities in outwardly propagating spherical syngas-air premixed flames. *International Journal of Hydrogen Energy*, *35*(8), 3868–3880. https://doi.org/10.1016/j.ijhydene.2010.01.091

Xie, Y., Wang, J., Xu, N., Yu, S., Zhang, M., & Huang, Z. (2014). Thermal and Chemical Effects of Water Addition on Laminar Burning Velocity of Syngas. *Energy & Fuels*, *28*(5), 3391–3398. https://doi.org/10.1021/ef4020586

8. RESPONSIBILITY NOTICE

The authors are the only responsible for the printed material included in this paper.